PCCP

Accepted Manuscript

This is an *Accepted Manuscript*, which has been through the Royal Society of Chemistry peer review process and has been accepted for publication.

Accepted Manuscripts are published online shortly after acceptance, before technical editing, formatting and proof reading. Using this free service, authors can make their results available to the community, in citable form, before we publish the edited article. We will replace this *Accepted Manuscript* with the edited and formatted *Advance Article* as soon as it is available.

You can find more information about *Accepted Manuscripts* in the Information for Authors.

Please note that technical editing may introduce minor changes to the text and/or graphics, which may alter content. The journal's standard Terms & Conditions and the Ethical guidelines still apply. In no event shall the Royal Society of Chemistry be held responsible for any errors or omissions in this *Accepted Manuscript* or any consequences arising from the use of any information it contains.

ROYAL SOCIETY OF CHEMISTRY

www.rsc.org/pccp

Correlation and mechanism of lithium ion diffusion with crystal structure in $Li_7La_3Zr_2O_{12}$ revealed by internal friction technique

X.P. Wang✉, Y.X. Gao, Y.P. Xia, Z. Zhuang, T. Zhang, Q.F. Fang

Key Laboratory of Materials Physics, Institute of Solid State Physics, Chinese Academy of Sciences, Hefei 230031, P.R. China

Abstract: The correlation and transport mechanism of lithium ions with crystal structure in fast lithium ion conductor $Li_7La_3Zr_2O_{12}$ are mainly investigated by internal friction (IF) and AC impedance spectroscopy techniques. Compared with the poor conductivity of tetragonal $Li_7La_3Zr_2O_{12}$, the Al stabilized cubic phase exhibits a good ionic conductivity that can be up to 1.9×10^{-4} S/cm at room temperature, which can be ascribed to the disordered distribution of lithium ions in the cubic phase. A well-pronounced relaxation IF peak (labeled as peak P_C) is observed in the cubic phase while a very weak IF peak (labeled as P_T) is observed in the tetragonal phase, further evidencing the difference of lithium ion migration in the two phases. Peak P_C can be decomposed into two sub-peaks with the activation energy and pre-exponential factor of relaxation time being E_1=0.41 eV, $\tau_{01}=1.2\times10^{-14}$s for the lower temperature peak P_{C1} and E_2 =0.35 eV, $\tau_{02}=1.9\times10^{-15}$s for the higher temperature P_{C2} peak, respectively. Based on the crystalline structure of cubic garnet-type $Li_7La_3Zr_2O_{12}$ compound, an atomistic mechanism of lithium ion diffusion via vacancies is suggested, i.e. 48*g*(96*h*)↔48*g*(96*h*) for peak P_{C1} and 48*g*(96*h*)↔24*d* for peak P_{C2}, respectively. The weak P_T peak in the tetragonal phase is preliminarily interpreted as the short jump process among neighbor octahedral sites and vacant tetrahedral sites.

✉ Corresponding author. Tel: +86-551-65591125; Fax: +86-551-65591434, *E-mail*: xpwang@issp.ac.cn

Physical Chemistry Chemical Physics Accepted Manuscript

Physical Chemistry Chemical Physics Accepted Manuscript

1. Introduction

Rechargeable all-solid-state lithium batteries have been considered as the next-generation high-performance power sources because of their remarkable advantages in battery miniaturization, energy density and battery safety compared with the already commercialized lithium ion batteries utilizing liquid or polymer-supported electrolytes. Li-rich oxides with garnet-like structure were initially developed as a novel family of solid state lithium electrolytes by Weppner et al [1-4], including $Li_5La_3M_2O_{12}$ (M=Ta, Nb, Bi), $Li_7La_3Zr_2O_{12}$ as well as the related cation-doped series. Among these garnet-related lithium electrolytes, $Li_7La_3Zr_2O_{12}$ attracted much attention because of its high lithium ionic conductivity but negligible electronic conductivity as solid electrolytes for lithium batteries [4].

The $Li_7La_3Zr_2O_{12}$ compound exhibits two different phase structures: cubic at high temperature and tetragonal at low temperature. In tetragonal $Li_7La_3Zr_2O_{12}$ with space group $I4_1/acd$, the lithium ions distributes in an ordered state, that is to say, all Li sites with same symmetry is either fully occupied or completely empty, resulting in a poor ionic conductivity (~10^{-6} S/cm at 300 K) [5]. In the high conductive cubic phase (space group *Ia*-3*d*), lithium ions distributes in a disordered state, that is, all Li sites with same symmetry is only partially occupied. The partial accommodation and disordered distribution of lithium ions lead to the high conductivity of cubic phase (~10^{-4} S/cm at 300 K) [6, 7]. So considering for the actual application as solid state electrolytes in lithium batteries, the cubic phase is preferred during the preparation of $Li_7La_3Zr_2O_{12}$ compound. But in general, partial cationic substitution such as Li by Al and Zr by Ta, Nb, Si, Ga or Y is necessary to stabilize the cubic phase to room temperature during sample preparation [6-8].

As viewed from the crystal structure of garnet-type compounds, the accommodation of lithium ions in lattices is noted to closely depend on lithium concentration. In the standard $A_3B_3C_2O_{12}$ garnet structure, the $B_3C_2O_{12}$ framework contains a 3D-connected interstitial space of tetrahedral sites (24*d*) that are bridged by empty face-sharing octahedral sites (48*g*). In the case of $Li_xB_3C_2O_{12}$ compounds with $x>3$, the tetrahedral 24*d* sites are not many enough to accommodate all Li^+ cations and the extra Li^+ must enter the octahedral 48*g* sites that are empty for the standard garnet structure. In this condition, the Li^+-Li^+ interaction across the shared 24*d*-48*g* face will displace the Li^+ ions from central octahedral sites (48*g*) to a position of 96*h*

sites near the opposite face [9]. It is worthy to point out that in garnet-type cubic $Li_7La_3Zr_2O_{12}$, the high concentration lithium vacancies are actually intrinsic owing to the partial accommodation in Li sub-lattice, which in turn makes cubic $Li_7La_3Zr_2O_{12}$ a good lithium ion conductor.

In solid state lithium electrolytes, the migration ability of lithium ions via vacancies plays a very crucial role for its conduction properties. So far, a number of researches based on experimental investigation and theoretical simulation were carried out to investigate the crystal structure and conductivity of the garnet-type oxides, but the underlying mechanism of lithium ion migration is still controversial, especially owing to the insufficiency of experimental evidence. The internal friction (designated as IF) is a measure of the materials ability to dissipate mechanical energy, which is manifested by stress-stain hysteresis in the case of cyclic loading. Generally, IF (Q^{-1}) can be written as [10]:

$$Q^{-1} = \frac{\Delta W}{2\pi W} \qquad (1)$$

where W is the maximum stored elastic energy during one cycle, ΔW is the corresponding energy dissipation during that cycle. As a technique sensitive to the ion migration, this method has been successfully employed to investigate the transport properties of lithium ions [11,12]. Different from the long range diffusion of lithium ions, the IF method can distinguish different short range migration process of point defects in detail, because different diffusion process of defects will be related with different characteristic IF peaks, which correspond to different peak position, peak shape as well as relaxation parameters. In this investigation, the IF method was mainly exploited to study the correlation and mechanism of lithium ion diffusion with crystal structure in $Li_7La_3Zr_2O_{12}$, and different relaxation-type IF peaks related with the short range diffusion of lithium ions were observed in the tetragonal and cubic phase. The microscopic mechanism of such IF peaks were discussed in detail based on a coupling model and the crystalline structure of $Li_7La_3Zr_2O_{12}$ compound, and two different diffusion routes of lithium ions in the cubic lattice were suggested.

2. Experimental procedure

The polycrystalline ceramic samples of $Li_7La_3Zr_2O_{12}$ in our investigation were prepared by conventional solid-state

Physical Chemistry Chemical Physics Accepted Manuscript

reaction method. The initial reaction materials are high purity $La(OH)_3$ (99.99%), Li_2CO_3 (99.9%), ZrO_2 (99.9%) and Al_2O_3(99.9%), respectively. To investigate the influence of phase structure on lithium ion diffusion, two kinds of samples were synthesized: one is tetragonal $Li_7La_3Zr_2O_{12}$, and the other is cubic $Li_7La_3Zr_2O_{12}$ stabilized by 1 wt% Al. The detailed synthesis processes have been reported in our previous work [13]. Crystalline phases of all the investigated $Li_7La_3Zr_2O_{12}$ samples were identified by X-ray diffraction analysis at room temperature using Cu-Kα radiation in the 2θ range from 10° to 70° with a step of 0.033°. The whole pattern matching refinement of the XRD patterns was performed using the Fullprof program based on the garnet-like structure [14], in which a pseudo-Voigt function was used as the profile function in the refinements.

To compare the difference of lithium ion migration between the cubic and tetragonal $Li_7La_3Zr_2O_{12}$ compounds, the measurement of ionic conductivity was isothermally collected in air on a computer-controlled Hioki 3531 Z-Hitester frequency response analyzer in the frequency range of 42 Hz to 5 MHz. The sintered cubic and tetragonal $Li_7La_3Zr_2O_{12}$ bulks have a typical size of about 10×10×1.5 mm^3 for the electrical measurement. The low frequency IF measurements were carried out on a computer-controlled torsion pendulum under the forced vibration mode, in which the measurements at five different frequencies were carried out by varying the driven frequency in one measurement run with a heating rate of 2 K/min. The bar samples for the IF measurement were sawed from the sintered dense disc with a dimension of about 27×1×1.5 mm^3, and the maximum torsion strain amplitude were kept at 2.5×10^{-5} in all the measurements.

3. Experimental results

3.1 Structural characterization

Figure 1(a) presents the room temperature powder XRD patterns of the Al-stabilized and un-stabilized $Li_7La_3Zr_2O_{12}$ compounds. The Al-stabilized $Li_7La_3Zr_2O_{12}$ exhibits a typical garnet-type structure with cubic symmetry and no other impurity phases are found in the XRD pattern. In contrast with the cubic phase, a significant tetragonal splitting is observed in the un-stabilized $Li_7La_3Zr_2O_{12}$, as evidenced by the enlarged local (213) and (426) diffraction lines in the insert. For the obtained cubic phase, the XRD profiles can be well indexed using space group *Ia*-3*d*, as shown in Fig.1(b), in which beside

Physical Chemistry Chemical Physics Accepted Manuscript

the experimental data (symbols), the calculated, Bragg positions and difference pattern of the Rieteld refinement from the XRD data are also presented. The lattice constants determined from the refinement are a=12.964(9) Å, which are consistent with the reported values of 12.975 Å [15]. As for the tetragonal phase, the lattice constants determined were similarly deduced as a=13.126(2)Å and c=12.675(8) Å with a cell ratio of c/a=0.9657, as reported in Ref.[13].

3.2 Ionic conductivity

Figure 2 shows the typical impedance plots obtained in the temperature range of 55-500°C in air for an Al-stabilized cubic $Li_7La_3Zr_2O_{12}$ sample. At low temperature region, for example at 55°C, two pressed semicircles are observed at the high frequency side in the Nyquist spectrum, which are contributed to the resistance of bulk and grain boundary, respectively. While only one incomplete arc is obtained in high temperature AC impedance spectra, in which both the grains and grain boundaries are overlapped with each other. At the lower frequency range, a typical polarized tail is observed in each AC spectroscopy, indicating that the investigated garnet-like $Li_7La_3Zr_2O_{12}$ compound is actually ionic conductor in nature [9, 16]. Noting that the bulk resistance and grain-boundary resistance are not obviously separated from each other from the impedance plots, the lithium ionic conduction properties of the $Li_7La_3Zr_2O_{12}$ compounds is evaluated by using total conductivity (bulk + grain boundary) in the investigated temperature range. Since no clear semicircles are observed in most of the AC impedance spectra, the total resistances (R_b+R_{gb}) are thus evaluated from the low frequency intercepts of the polarized tail with the real Z' axis. Then, the total conductivity σ can be deduced with $\sigma=d/SR$, where d is the thickness of the sample, $S$is the area of the electrolyte and R is the corresponding total resistance.

The total lithium ionic conductivity determined from the AC impedance spectra is about 1.9×10^{-4} S/cm at room temperature for the Al-stabilized cubic $Li_7La_3Zr_2O_{12}$. This magnitude of conductivity can be comparable to the reported value of 2.4×10^{-4} S/cm in the 1.3 wt% Al doped $Li_7La_3Zr_2O_{12}$ [17]. Fig.3 gives the temperature dependence of total conductivity of the cubic phase, in which a linear Arrhenius plot is obtained. According to the Arrhenius relation: $\sigma T=A\exp(-E_a/kT)$ (where A is the pre-exponential factor, E_a is the activation energy and T is the absolute temperature), the activation energy E_a for lithium ionic transport in the Al stabilized cubic $Li_7La_3Zr_2O_{12}$ is determined to be 0.36 eV. The obtained activation energy data is a typical value for lithium ion diffusion in cubic garnet-type lithium electrolytes. For example, a value of 0.34 eV was also reported in the 0.5wt% Al containing $Li_7La_3Zr_2O_{12}$ sample [18].

For convenient comparison, the Arrhenius plot of the tetragonal $Li_7La_3Zr_2O_{12}$ is especially presented in Fig.3 as a reference, and the lithium ionic conductivity of the polycrystalline tetragonal compound determined from the AC

Physical Chemistry Chemical Physics Accepted Manuscript

impedance spectra is only about 1.1×10^{-7} S/cm at room temperature. The poor conductivity implies that the tetragonal phase cannot be considered for practical application as electrolytes. The noted abrupt enhancement of conductivity in the temperature range 150°C~200°C was ascribed to a tetragonal-cubic phase transition that have been verified by thermal XRD measurements [13]. The underlying mechanism related with dramatic difference of the ionic conductivity was suggested to be originated from the different distribution state of lithium ions in the cubic and tetragonal phases [19]. In the cubic phase, the Li sub-lattice is always disordered, resulting in the existence of adequate intrinsic lithium vacancies to facilitate lithium migration. On the contrary for the tetragonal phase, the Li sub-lattice is always ordered, exhibiting a regularly ordered Li ion vacancy structure that accordingly leads to its poor migration property of lithium ions.

3.3 Internal friction (IF)

Figure 4 presents the IF (Q^{-1}) and the relative modulus (M) versus temperature T in the temperature range from -30 °C to 195 °C for the Al stabilized $Li_7La_3Zr_2O_{12}$ at five different frequencies of 0.2, 0.5, 1, 2 and 4 Hz, respectively. The heating rate during the measurement is kept at 2 K/min and the maximum torsion strain amplitude is about 20×10^{-6}. An obvious IF peak (labeled as P_C peak) is observed in the temperature spectra for each frequency, and the peak height of the IF peak is as high as 0.10. The peak position is located around 59 °C at 1 Hz, accompanied by a corresponding decrease in modulus. The peak position gradually shifts to higher temperature with increasing frequency, while the peak height or relaxation strength hardly changes.

Fig.5 gives the temperature dependence of the IF (Q^{-1}) of the Al stabilized $Li_7La_3Zr_2O_{12}$ sample under four different experimental strain of 5, 10, 15 and 20×10^{-6}, respectively. The experimental results evidences that the IF spectra are matched very well under each strain magnitude in the whole measuring temperature range, which clearly indicates that relaxation strength of P_C peak is independent on strain magnitude. Such typical relaxation characteristics related with peak position, relaxation strength and strain magnitude demonstrates that P_C peak is associated with a thermally activated relaxation process [10].

In Fig.6, the IF (Q^{-1}) and the relative modulus (M) versus temperature T for an un-doped $Li_7La_3Zr_2O_{12}$ sample at four different frequencies are also presented, and a weak IF peak (labeled as P_T peak) located around 53°C at 1Hz is observed. This peak similarly shifts towards higher temperature with increasing frequency, indicating the relaxation characteristic of this peak. After subtracted the IF background, the peak height of the P_T peak is only about 0.01, which is much smaller than the value of 0.10 in the Al stabilized cubic phase. As a comparison, Fig.7 specially gives the IF spectra of the tetragonal and cubic $Li_7La_3Zr_2O_{12}$ at a same frequency of 1 Hz, in which the difference of peak height between the two phases is

Physical Chemistry Chemical Physics Accepted Manuscript

distinguished clearly. Carefully analyzing the IF spectra of the tetragonal phase, it is noted that the IF data at the higher temperature side fluctuates abnormally. Such instability of the IF data should be associated with the tetragonal-cubic phase transition in the temperature range of 150-200^{o}C, as confirmed by the thermal XRD analysis and conduction measurement. Since the tetragonal-cubic phase transition in the tetragonal $Li_7La_3Zr_2O_{12}$ is a gradual process, the fluctuation of IF data therefore covers a wide temperature range.

According to the theory of point defect relaxation, the relaxation strength has a linear dependence on the defect concentration and the square of the dipole shape factor based on the concept that each point defect (e.g. vacancy) behaves like an elastic dipole [10]. So the strong IF peak in the Al contained cubic $Li_7La_3Zr_2O_{12}$ (about 0.10) means a high concentration of relaxation species that participate in the diffusion process. On the contrary, the weak relaxation peak (only 0.01) in the tetragonal phase corresponds to a very low concentration of relaxation species. But with regard to the relaxation essence, the similar relaxation characteristic as well as peak position implies that peak P_C and peak P_T are most possibly related with a same relaxation mechanism.

In solid materials, the short-range diffusion of atoms or vacancies, such as oxygen ions and lithium ions as well as the corresponding vacancies, can be described as the reorientation of the dipoles [10,11]. Therefore the migration processes of atoms or vacancies would give rise to relaxation peaks when an oscillating stress field is applied. As for the $Li_7La_3Zr_2O_{12}$ compounds, the cations such as La and Zr that constructed the rigid lattice of the compounds, have no possibility to migrate at room temperature owing to the high diffusion energy. The full accommodation of oxygen ions cannot provide enough vacancies to induce such a high peak, either. Therefore, the most possible mechanism related with the relaxation peaks in $Li_7La_3Zr_2O_{12}$ is thus ascribed to the short-range diffusion of lithium ions via vacancies because the point defects (e.g. lithium vacancies) behave like not only an electric dipole but also an elastic dipole.

It is worthy to note that in cubic $Li_7La_3Zr_2O_{12}$ phase [19], the migration of high concentration lithium ions via vacancies leads to good conductivity at room temperature; whereas in the tetragonal phase, the low crystalline symmetry and ordered distribution of lithium ions result in a poor ionic conductivity. Based on this consideration, the obvious difference of relaxation strength of the IF peaks can be interpreted as the different concentration of mobile lithium ions (or vacancies) in the cubic and tetragonal $Li_7La_3Zr_2O_{12}$. In the tetragonal phase, the ordered distribution of lithium means that the Li sites are either fully occupied or empty in lithium sub-lattice, leading to the absence of adequate amount of lithium vacancies that would make the lithium ions immobile. Benefiting from the disordered distribution of lithium ions in cubic phase, the most lithium ions are mobile because of the existence of high concentration intrinsic lithium vacancies that correspond to the high ionic conductivity and the strong relaxation IF peak. Since the diffusion ability in tetragonal

Physical Chemistry Chemical Physics Accepted Manuscript

$Li_7La_3Zr_2O_{12}$ is relatively low, the following discussion will be mainly focused on the diffusion process and mechanism of lithium ions in the Al stabilized cubic $Li_7La_3Zr_2O_{12}$ electrolyte.

4. Discussion

4.1 Nonlinear fitting method of internal friction spectroscopy based on coupling model

In lithium electrolytes, the diffusion processes of lithium ions are not isolated but collaborative in nature owing to the strong mutual interaction among high concentration lithium ions. It is well known that the coupling model is a proper candidate model to phenomenologically describe this kind of mutual interaction [20, 21]. According to this model, the correlation function $C(t)$ can be separated into two regions by a temperature-independent crossover time t_c, that is,

$$C(t) = \exp(-t/\tau) \quad \text{for } t< t_c \tag{2}$$

$$C(t) = \exp[-(t/\tau^*)^{\beta}] \quad \text{for } t> t_c \tag{3}$$

Here β is a coupling parameter that is an indicator of the degree of correlation in the relaxation process originating from the mutual interactions ($0 < \beta \leq 1$) and decreases as the coupling strength increases; τ^* and τ are the coupled relaxation time and decoupled relaxation time, respectively. According to the neutron-scattering experiments and molecular-dynamics simulations, the magnitude of t_c is in the order of 10^{-11}~10^{-12}s for amorphous polymers, and 10^{-12}~10^{-13}s for metals and ionic conductors [22]. Further based on the continuity of relaxation functions, there is

$$\tau=t_c^{1-\beta}\tau^{*\beta} \tag{4}$$

Combining the so-called Arrhenius law ($\tau=\tau_0\exp(E/kT)$ (where k is the Boltzmann constant, E is the activation energy, and T is the absolute temperature) with equation (4), we have

$$E=\beta E^* \tag{5}$$

$$\ln(\tau_0)=\beta\ln(\tau_0^*)+(1-\beta)\ln(t_c) \tag{6}$$

where E^* and E are the coupled and decoupled activation energies, τ_0^* and τ_0 are the pre-exponential factors of coupled and decoupled relaxation time, respectively.

On the other hand according to the definition of internal friction, the IF (Q^{-1}) can be expressed by the compliances [10]:

$$Q^{-1}(\omega)=J_2(\omega)/J_1(\omega) \tag{7}$$

where ω is the circular frequency, J_1 and J_2 are the real and imaginary parts of the complex compliance $J(\omega)$, respectively,

Physical Chemistry Chemical Physics Accepted Manuscript

and $J(\omega)=J_1(\omega)-iJ_2(\omega)$. If the interaction of relaxation species is considered, J_1 and J_2 can be mathematically expressed as follows [23]:

$$J_1(\omega) = J_U + \beta\delta J \int_0^\infty z^{\beta-1}\exp(-z^\beta)\cos(\omega\tau^* z)dz \quad (8)$$

$$J_2(\omega) = \beta\delta J \int_0^\infty z^{\beta-1}\exp(-z^\beta)\sin(\omega\tau^* z)dz \quad (9)$$

where β is the correlation parameter mentioned above, and $z=t/\tau^*$, $\delta J=J_R-J_U$ (J_R, J_U are the relaxed and unrelaxed compliance, respectively). Thus using Eqs. (7-9), the IF as functions of β and $\omega\tau^*$ can be calculated. Further in terms of Arrhenius relation $\tau=\tau_0\exp(E/kT)$, the IF experimental data are generally fitted as functions of β and $1/T$ at a constant frequency for convenience.

4.2 Activation parameters of lithium ion diffusion in $Li_7La_3Zr_2O_{12}$

In the investigation of Al stabilized cubic $Li_7La_3Zr_2O_{12}$, the existence of mutual interaction among lithium ions can be further confirmed from the wide IF peak, as shown in Fig.8(a), in which the relaxation peak P_C is found to be obviously broader than a standard Debye peak, and the obvious mismatch is observed at the lower temperature, implying the existence of another subpeak. Using the coupling model combined by a nonlinear fitting method of IF spectrum mentioned above, the prominent IF peak observed in the cubic $Li_7La_3Zr_2O_{12}$ can be well fitted by two sub-peaks, as shown in Fig.8(b), in which the fitting result of the IF peak measured at 1 Hz is particularly presented as an example, and the value of t_c was taken as 10^{-12}s during the fitting process. For clear description, the lower temperature sub-peak with a height of 0.01 was denoted by peak P_{C1} and the higher temperature sub-peak with a height of 0.09 was denoted by P_{C2}, and the corresponding coupling parameter β is determined as 0.45 and 0.27, respectively. The relatively low value for the coupling parameter β further demonstrates the strong mutual interaction among diffusion lithium ions.

Through the nonlinear fitting of the IF curves, the peak temperature (T_P) of the two sub-peaks under different measuring frequencies can be precisely determined, and the corresponding coupled activation energy E^* and the pre-exponential factor τ_0^* can be thus obtained in terms of the shift of peak temperature with measuring frequency. In Fig.9, the corresponding Arrhenius plots of the two relaxation sub-peaks are presented, where the solid lines are the linear least-square fittings. Base on the Arrhenius relation, the coupled relaxation parameters E^* and τ_0^* deduced from the slope

Physical Chemistry Chemical Physics Accepted Manuscript

and intercept of the ln(ω)-1/T_p lines are determined as E_1*=0.91 eV, τ_{01}*=5.2×10^{-17}s for the peak P_{C1} and E_2* =1.3 eV, τ_{02}* =1.9×10^{-22}s for the P_{C2} peak, respectively. By substituting the coupling parameter β and the coupled relaxation parameter E*, τ_0* into equation (5) and (6), the decouple relaxation parameters are determined as E_1=0.41 eV, τ_{01}=1.2×10^{-14}s for the peak P_{C1} and E_2 =0.35 eV, τ_{02}=1.9×10^{-15}s for the P_{C2} peak, respectively, as shown in Table 1. As a comparison, the Arrhenius plot of peak P_T is also presented. The peak positions of peak P_T at different frequencies are close to that of peak P_{C1} and the activation energy of peak P_T is determined as 1.05 eV.

The obtained decoupled τ_0 for the IF peak in the order of 10^{-14}~10^{-15} falls in the range of typical values for processes of point defect relaxation. Moreover, the decoupled activation energy of both peaks in the range of 0.35-0.41 eV is also in good agreement with the value of 0.36 eV for lithium ion diffusion obtained in forgoing conduction measurement. This result demonstrates that the coupling model is suitable to describe the relaxation process of lithium diffusion in the $Li_7La_3Zr_2O_{12}$ compound. From another side, the comparable relaxation parameters between the IF and conductivity measurement also provide a convincing evidence about mechanism of the relaxation IF peaks, which are related with the diffusion of lithium ions via vacancies. Different from the average effect in conductivity related with long distance migration of carriers, the IF peaks reflect the short diffusion processes of lithium ions under periodic stress. The coexistence of two sub-peaks reveals from experimental aspects that there should be at least two different routes for lithium ion migration in the lithium sub-lattice of the cubic $Li_7La_3Zr_2O_{12}$ oxide based on the consideration of one IF peak corresponding to one kind of relaxation process.

4.3 Diffusion mechanism of lithium ions in cubic $Li_7La_3Zr_2O_{12}$ crystal

In the garnet-type cubic $Li_7La_3Zr_2O_{12}$ lattice, La^{3+} ions occupy the eight-coordinate sites, and Zr^{4+} ions stay on the six-coordinate octahedral sites, and there are two possible sites to accommodate Li ions [18]: tetrahedral 24*d* (labeled as Li(I)) and octahedral 48*g* (labeled as Li(II)). In the case of occupation positions deviating from octahedral center, the octahedral Li(II) sites are usually called as 96*h* because they are still inside the Li(II) octahedra. Since the possible accommodation sites are more than the total amount of lithium ions in each $Li_7La_3Zr_2O_{12}$ super-cell, the Li(I) and Li(II) sites are partially occupied, which were about 88% occupied in octahedral Li(II) sites and about 56% occupied in

Physical Chemistry Chemical Physics Accepted Manuscript

tetrahedral Li(I) sites, as experimentally predicted by neutron diffraction patterns [19]. The *ab*-initio calculations further revealed that most of Li(II) ions actually displaced off their original central 48*g* sites, approaching the 96*h* sites because of the Coulombic interaction [24]. The displacement from the 48*g* octahedral geometric center increases the average separation among octahedral sites up to about 2.5307Å, obviously larger than the Li(I)-Li(II) separation which is only about 1.9898Å [25].

Figure 10(a) presents the crystal structure model of cubic $Li_7La_3Zr_2O_{12}$ projected on (001) direction (space group *Ia*-3*d*, a=13.126Å), which is based on the refinement result of the X-ray diffraction pattern collected at room temperature using Cu-Kα radiation, and Fig.10(b) and (c) give the 2D schematics of the Li accommodation, in which either 24*d* or adjacent 96*h* sites is occupied because Coulombic repulsion energetically prohibited the simultaneous occupation of the two kinds of sites [19]. According to the thermodynamic selection rule for point defect relaxation, such processes may occur for those point defects whose symmetry is lower than that of the crystal. In the cubic $Li_7La_3Zr_2O_{12}$ crystal, all of the lithium sites have this lower symmetry. Therefore, an IF peak may be resulted from one migration process between the following three pairs when only the jumps between the nearest neighbors are considered:

$$24d \leftrightarrow 24d \qquad 48g(96h) \leftrightarrow 24d \qquad 48g(96h) \leftrightarrow 48g(96h)$$

Further considering the structural framework, the interstitial tetrahedral sites (24*d*) are surrounded by face-sharing octahedral sites, which actually excludes the possibility of direct diffusion among the neighbor tetrahedral Li(I) sites. Therefore, the diffusion routes for lithium lions in cubic $Li_7La_3Zr_2O_{12}$ have only two possibilities: 48*g*(96*h*)↔24*d* and 48*g*(96*h*)↔48*g*(96*h*). According to this schematics, two kinds of possible diffusion routes of lithium ions are proposed in Fig.10(b) and Fig.10(c): one is via the 24*d* tetrahedral site, i.e. 48*g*(96*h*)↔24*d*, and the other is between neighboring octahedral Li(II)-Li(II) sites bypassing the tetrahedral Li(I) neighbors, i.e. 48*g*(96*h*)↔48*g*(96*h*). The investigation of high-temperature neutron diffraction coupled with maximum-entropy method also predicted a 3D diffusion pathway of lithium ions consisting of the following interlocking chain segments [26]: Li(24*d*)-Li(96*h*)-Li(48*g*)-Li(96*h*)- Li(24*d*).

During the above analysis of IF results, the wide peak P_C is decomposed into two sub-peaks, P_{C1} and P_{C2}, which are suggested to originate from different migration routes. It is therefore very interesting to discuss the relation of the IF peaks with diffusion routes of lithium ions. In terms of the crystal structure of $Li_7La_3Zr_2O_{12}$, the tetrahedral Li(I) sites are surrounded by face-sharing octahedral 48*g* sites, once the Li(I) sites are unoccupied, the diffusion of lithium ions between 96*h* and 24*d* is relatively easy owing to the short diffusion distance (~1.9898Å) as well as the low diffusion barrier (~0.3-0.4 eV). On the contrary for the jump of lithium ions among the neighbor 48*g* (or 96*h*) sites, it is relatively difficult because of its longer diffusion distance (~2.5307Å) and higher diffusion activation energy [25]. The energy barrier among the neighbor

Physical Chemistry Chemical Physics Accepted Manuscript

48*g* sites can be even as high as 0.8 eV in the garnet-type compounds, for example $Li_5La_3Nb_2O_{12}$, as determined by dynamic simulation on lithium ion diffusion [24]. Besides that, the Li(I) ions are unstable at tetrahedral sites and consequently tend to migrate to neighboring octahedral sites, which result in much more pronounced Li residence at the 48g/96h sites (~88%) than at the 24d sites (~56%) [19]. The lower occupation in tetrahedral Li(I) sites would provide more diffusion possibility of lithium ions between 96*h* sites and 24*d* site in comparison with the higher occupation rate in octahedral Li(II) sites.

Since the relaxation strength of the IF peak is linearly dependent on the concentration of mobile lithium ions or vacancies, the mechanism of the weak P_{C1} component at lower temperature is suggested to be originated from the jump process among the neighboring octahedral Li(II) sites, i. e. 48*g*(96*h*)↔48*g*(96*h*), because of the higher diffusion barrier and lower vacancy concentration at 48*g*(96*h*) sites, as shown in Fig.10(b). Accordingly for the strong P_{C2} component at higher temperature, its mechanism most possibly originates from jumping process among the nearest octahedral Li(II) sites and tetrahedral Li(I) sites i. e. 48*g*(96*h*)↔24*d*, owing to its lower diffusion barrier and higher vacancy concentration at 24*d* sites. By using *ab*-initio based molecular dynamics [25], Jalem *et al* concluded that the jump of lithium ion is actually simultaneous among different Li sites including the case for cooperative motion in Li(II)-Li(I)-Li(II) trimers as well as different Li(II)-Li(II) dimers, which is consistent with the coupling model that was used to obtain the decoupled relaxation parameters of lithium ion diffusion. Further considering from the cubic symmetry of $Li_7La_3Zr_2O_{12}$, the diffusion process of lithium ions via vacancies is 3-dimensional in nature, the long distance diffusion of lithium ions may be possible through the path of Li(24*d*)-Li(96*h*)-Li(48*g*)-Li(96*h*)-Li(24*d*), as proposed by Han *et al* [26]. Such theoretical analyses are actually well matched with our IF experimental results.

In the tetragonal $Li_7La_3Zr_2O_{12}$, there are three possible sites for Li accommodation in lattice, which are characterized by tetrahedral 8*a*, octahedral 16*f* and octahedral 32*g*, respectively. Different from the partial and disordered occupation of 24*d* and 48*g*(96*h*) site in the cubic phase, the three different Li sites in the tetragonal phase are actually ordered and fully occupied, resulting in two-thirds of the tetrahedral sites being kept vacant while octahedral sites being fully occupied [5]. The fully accommodation in the octahedral 16*f* and 32*g* sites limits the migration among the octahedral sites because of the absence of lithium vacancies. Therefore, the relaxation mechanism of peak P_T in the tetragonal $Li_7La_3Zr_2O_{12}$ is most possibly related with diffusion process among neighbor octahedral sites and vacant tetrahedral sites. As for the weak relaxation strength (~0.01) for peak P_T, it is owing to the ordered distribution of lithium ions and vacancies in the tetragonal phase.

Physical Chemistry Chemical Physics Accepted Manuscript

Such stable and ordered distribution tends to keep lithium ions immobile in these positions. Thus the lack of mobile Li ions will therefore leads to the weak IF peaks as well as poor ionic conductivity in the tetragonal phase. However, to clearly understand the relaxation process and microscopic mechanism related with the diffusion of lithium ions via vacancies in the $Li_7La_3Zr_2O_{12}$ electrolytes, further theoretical analysis based on the crystal structure is necessary, not only for the tetragonal phase but also for the cubic phase.

5. Conclusion

Conduction properties and diffusion mechanism of lithium ions in the tetragonal and 1wt% Al stabilized cubic $Li_7La_3Zr_2O_{12}$ compounds are systematically investigated by AC impedance spectroscopy and IF methods. The conduction measurement shows that the conductivity of the stabilized cubic phase can be up to1.9×10^{-4} S/cm at room temperature, this value is about three orders of magnitude higher than that of the tetragonal phase. Benefiting from a tetragonal-cubic phase transformation in the temperature range 150°C~200°C, the conductivity of the tetragonal phase is found to be greatly enhanced owing the ordered-disordered transition of lithium ion distribution.

The IF results further evidenced the difference of lithium ion migration associated with the phase structure for the $Li_7La_3Zr_2O_{12}$ oxides, in which a well-pronounced relaxation IF peak with peak height of about 0.10 was observed in the cubic phase, while the relaxation strength of the IF peak in the tetragonal phase was only about 0.01. Considering that the IF peak was induced by lithium ion diffusion, the different IF behaviors in the cubic and tetragonal phases are similarly ascribed to the different distribution of lithium ions in lattice.

By using a coupling model, the prominent peak *P*c was well decomposed into two components: P_{C1} and P_{C2} peaks. The activation energy and pre-exponential factor of relaxation time of these two peaks are E_1=0.41 eV, $\tau_{01}=1.2\times10^{-14}$s for the peak P_{C1} and E_2 =0.35 eV, $\tau_{02}=1.9\times10^{-15}$s for the P_{C2} peak, respectively. Such relaxation parameters are in good agreement with the obtained results in conduction measurement. Based on the crystal structure of cubic $Li_7La_3Zr_2O_{12}$, the P_{C1} and P_{C1} peaks are suggested to be originated from two kinds of short-distance diffusion of lithium ions between different sites, i.e. 48*g*(96*h*)↔48*g*(96*h*) and 48*g*(96*h*)↔24*d,* respectively. A possible path of long distance diffusion of lithium ions was

Physical Chemistry Chemical Physics Accepted Manuscript

suggested in terms of Li(24*d*)-Li(96*h*)-Li(48*g*)-Li(96*h*)-Li(24*d*) chain segments, which is 3-dimensional in nature. As for the weak P_T peak in the tetragonal phase, the mechanism is preliminary interpreted as the short jump process among neighbor octahedral sites and vacant tetrahedral sites. The obtained experimental results also confirmed that different from the average behavior of conductivity, the IF method can be used as a sensitive and potential probe to explore the local diffusion process of carriers in detail in solid lithium electrolytes.

Acknowledgments

This work was subsidized by the National Natural Science Foundation of China (Grant Nos: 11374299, 11274305, 11174283).

Physical Chemistry Chemical Physics Accepted Manuscript

Reference

[1] V. Thangadurai, H. Kaack and W. J . F. Weppner, *J. Am. Ceram. Soc.,* 2003, **86**, 437.

[2] R.Murugan, W. Weppner and P. Schmid-Beurmann, *Mater. Sci. Eng. B* 2007, **143**, 14.

[3] V. Thangadurai and W. Weppner, *J. Solid State Chem*., 2006, **179**, 974.

[4] M. Ramaswamy, T. Venkataraman and W. Weppner, *Angew. Chem. Int. Ed*., 2007, **46**, 7778.

[5]K. Junji, K. Norihito, H. Hiroshi and J. Akimoto , *J. Solid State Chem*., 2009, **182**. 2046.

[6] J. L. Allen, J. Wolfenstine, E. Rangasamy and J. Sakamoto, *J. Power Sources* 2012, **206**, 315.

[7] M. Huang, A. Dumon and C. W. Nan, *Electrochem. Comm*., 2012, **21**, 62.

[8] Y. Jin and P. J. Mcginn, *J. Power Sources* 2011, **196**, 8683.

[9] Y. T. Li, J. T. Han, C. A. Wang, S. C. Vogel, H. Xie, M. W. Xu and J. B. Goodenough, *J. Power. Sources* 2012, **209**, 278.

[10] A. S. Nowick and B. S. Berry BS, in *Anelastic Relaxation in Crystalline Solids*, Academic Press, New York and London, 1972.

[11] X. P. Wang, W. G. Wang, Y. X. Gao, T. Zhang and Q. F. Fang, *Mater. Sci. Eng. A* 2009,**521-522**, 87.

[12] Y. X. Gao, Z. Zhuang, H. Lu, X. P. Wang and Q. F. Fang, *Solid State Phenomena* 2012,**184**,116.

[13] X. P. Wang, Y. Xia, J. Hu, Y. P. Xia, Z. Zhuang, L. J. Guo, H. Lu, T. Zhang and Q. F. Fang, *Solid State Ionics* 2013, **253**, 137.

[14] J. Rodrguez-Carvajal, *Physica (Amsterdam)* 1993, **192B**, 55.

[15]C. A. Geiger, E. Alekseev, B. Lazic, M. Fisch, T. Armbruster, R. Langner, M. Fechtelkord, N. Kim, T. Pettke, and W.Weppner, *Inorg. Chem* 2011, **50**, 1089

[16] N. Janani, S. Ramakumar, L. Dhivya, C. Deviannapoorani, K. Saranya and R. Murugan, *Ionics* 2011, **17**, 575.

[17] S. Kumazaki, Y. Iriyama, K. H. Kim, R. Murugan, K. Tanabe, K. Yamamoto, T. Hiryama and Z. Ogumi, *Electrochem. Commun* ., 2011, **13**, 09.

[18] H. Buschmann, J. Dölle, S. Berendts, A. Kuhn, P. Bottke, M. Wilkening, P. Heitjans, A. Senyshyn, H. Ehrenberg, A.

Physical Chemistry Chemical Physics Accepted Manuscript

Lotnyk, V. Duppel, L. Kienle and J. Janek, *Phys. Chem. Chem. Phys.,* 2011, **13**, 19378.

[19] H. Xie, J. A. Alonso, Y. T. Li, M. T. Fernández-Díaz and J. B. Goodenough, *Chem. Mater.,* 2011, **23**, 3587.

[20] K. L. Ngai , in *Disorder Effects on Relaxation Processes*, Springer-Verlag, Heidelberg, 1994.

[21] K. L. Ngai, Y. N. Wang and L. B. Magalas, *J. Alloys Comp*., 1994, **211-212**, 327.

[22] K. L.Ngai, H.Jain H, *Solid State Ionics* 1986, **18-19**, 362.

[23] Y. Shi,W. B. Jiang, Q. P. Kong, P. Cui, Q. F. Fang and M. Winning, *Phys. Rev. B* 2006, **73**,174101.

[24] M. Xu, M. S. Park, J. M. Lee, T. Y. Kim, Y. S. Park and E. Ma, *Phys. Rev. B* 2012, **85**, 052301.

[25] R. Jalem, Y. Yamamoto, H. Shiiba, M. Nakayama, H. Munakata, T. Kasuga and K. Kanamura, *Chem. Mater.,* 2013, **25,** 425.

[26] J. T. Han, J. L. Zhu, Y. T. Li, X. H. Yu, S. M. Wang, G. Wu, H. Xie, S. C. Vogel, F. Lzumi, K. Momma, Y. Kawamur, Y. H. Huwang, J. B. Goodenough andY. S. Zha, *Chem. Commun* 2012, **48**, 9840.

Physical Chemistry Chemical Physics Accepted Manuscript

Table 1: The coupling and activation relaxational parameters for P_{C1} and P_{C2} subpeaks, respectively.

	E^*(eV)	τ^*_0 (s)	β	E (eV)	τ_0 (s)
P_1 peak	0.91	5.2×10^{-17}	0.45	0.41	1.2×10^{-14}
P_2 peak	1.30	1.9×10^{-22}	0.27	0.35	2.4×10^{-15}

Physical Chemistry Chemical Physics Accepted Manuscript

Figure 1 by X. P. Wang, *et al*

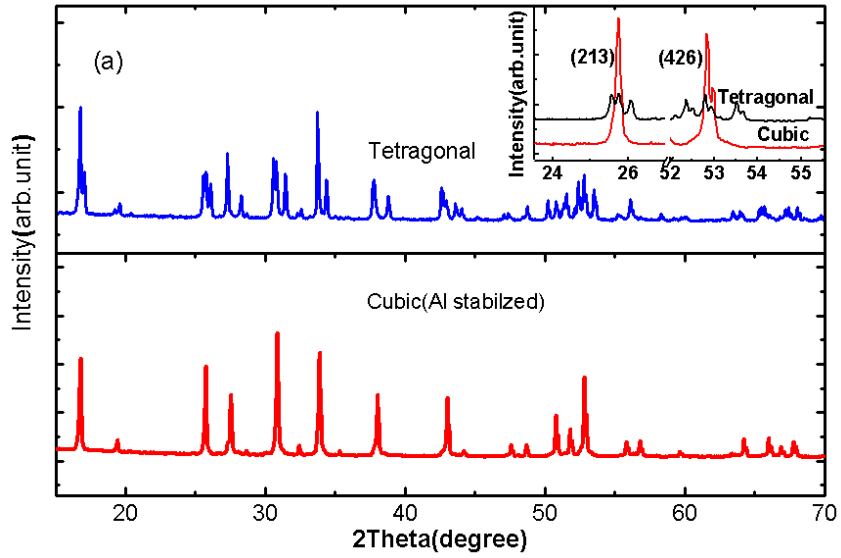

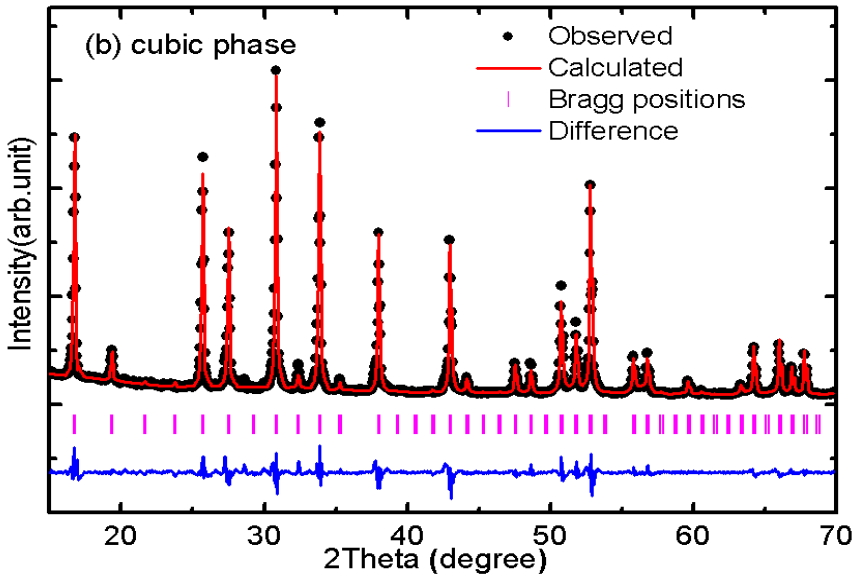

Physical Chemistry Chemical Physics Accepted Manuscript

Figure 2 by X. P. Wang, *et al*

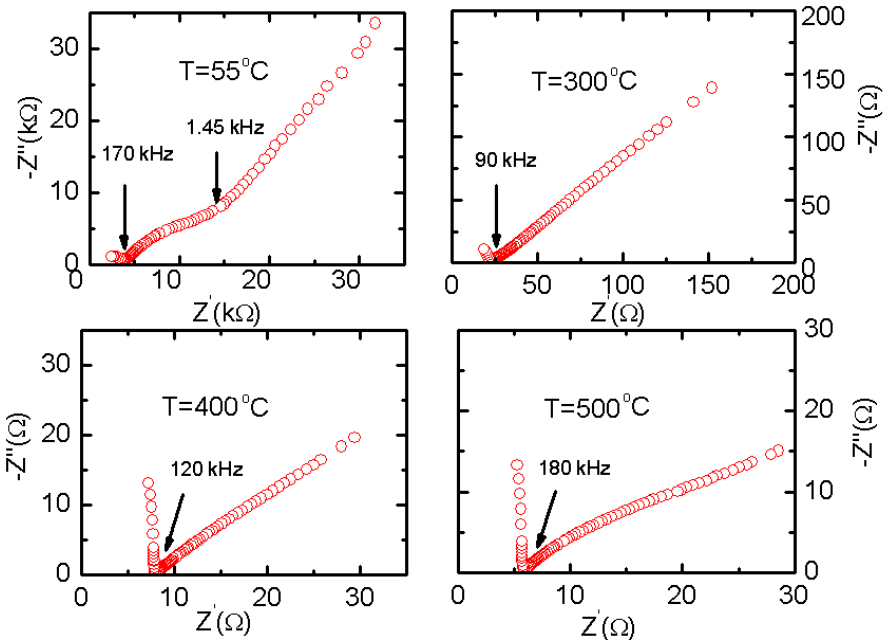

Figure 3 by X. P. Wang, *et al*

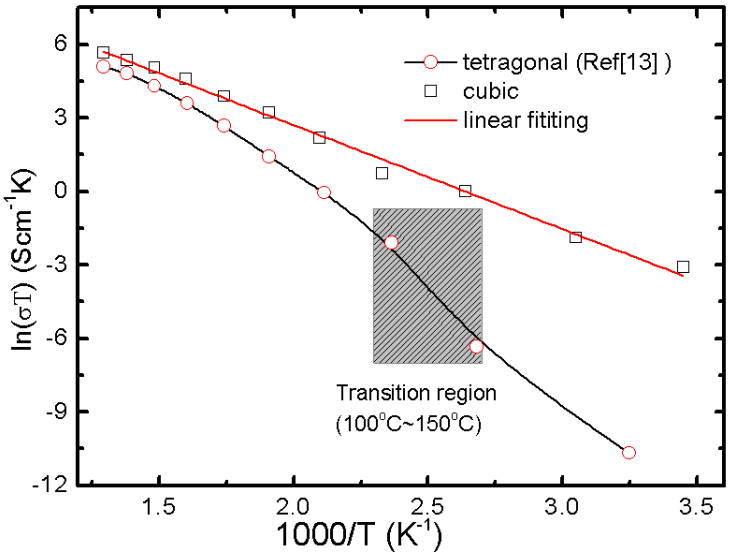

Physical Chemistry Chemical Physics Accepted Manuscript

Figure 4 by X. P. Wang, *et al*

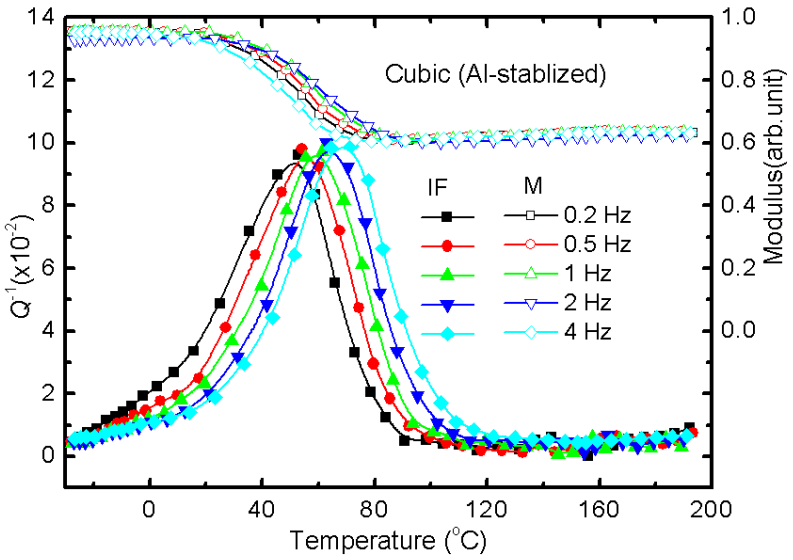

Figure 5 by X. P. Wang, *et al*

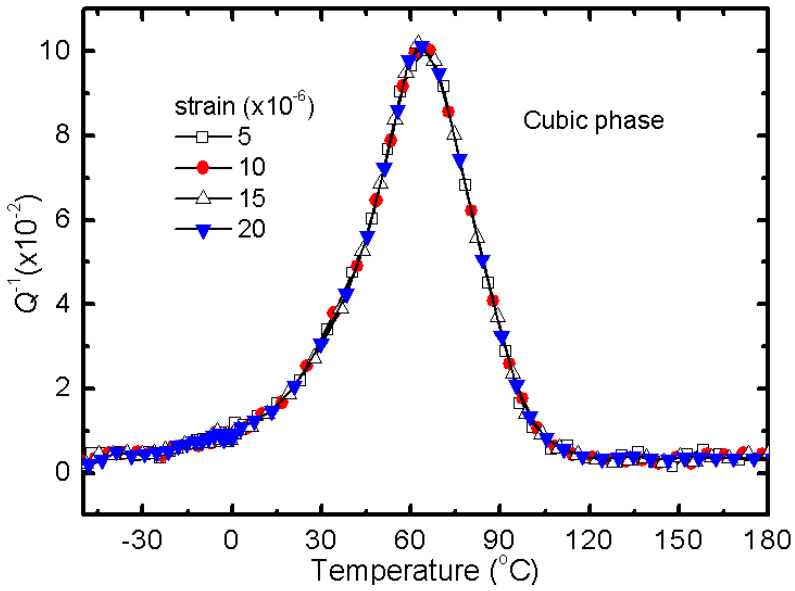

Physical Chemistry Chemical Physics Accepted Manuscript

Figure 6 by X. P. Wang, *et al*

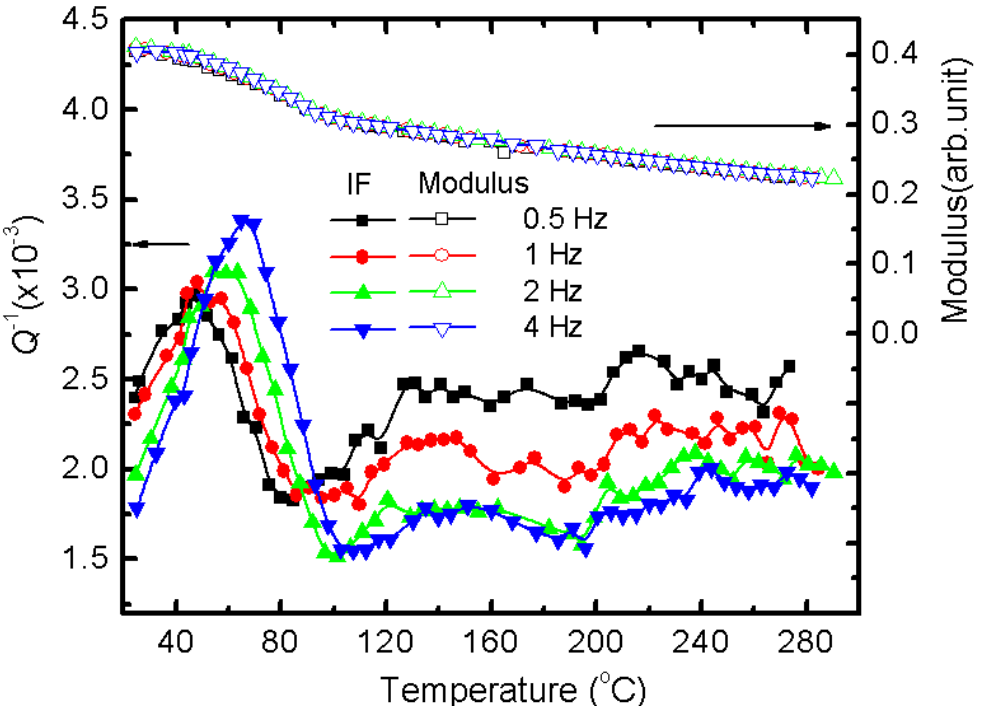

Figure 7 by X. P. Wang, *et al*

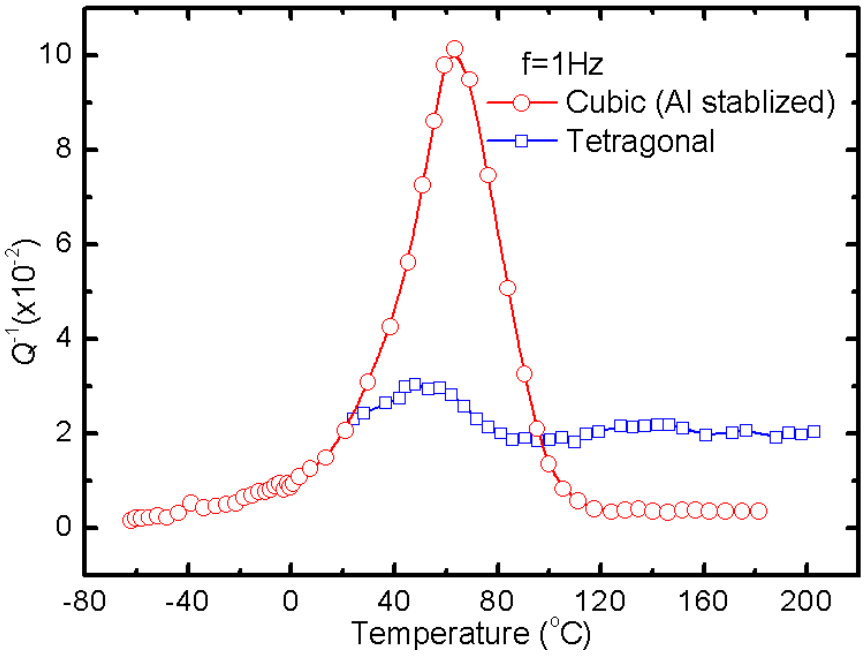

Physical Chemistry Chemical Physics Accepted Manuscript

Figure 8 by X. P. Wang, *et al*

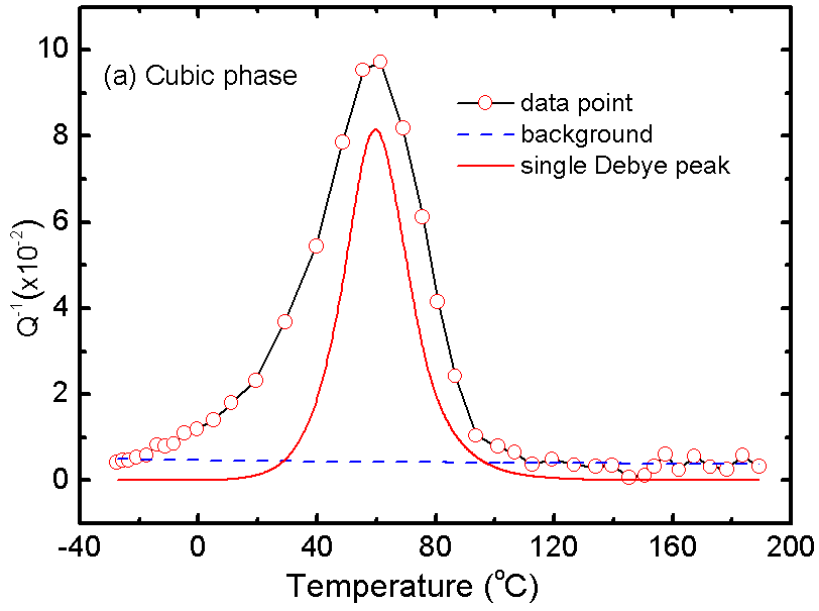

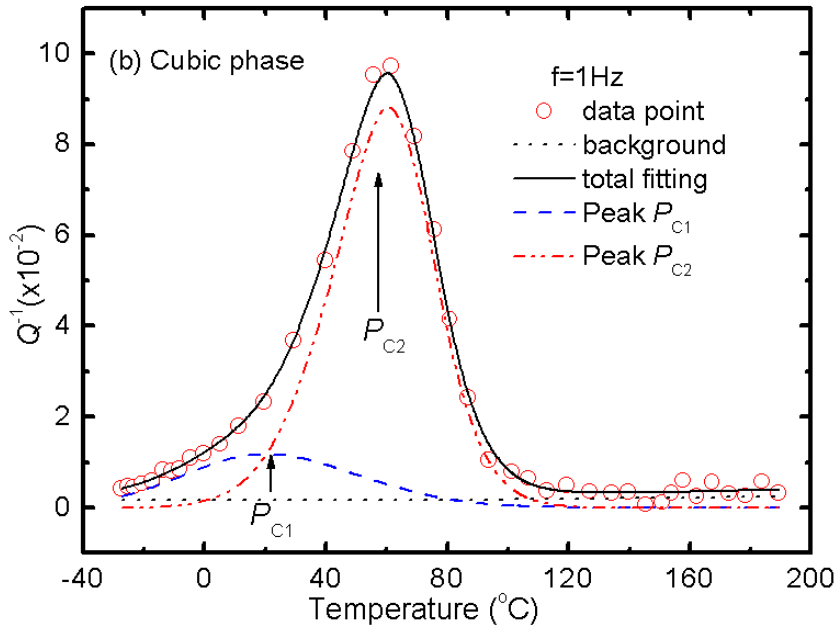

Physical Chemistry Chemical Physics Accepted Manuscript

Figure 9 by X. P. Wang, *et al*

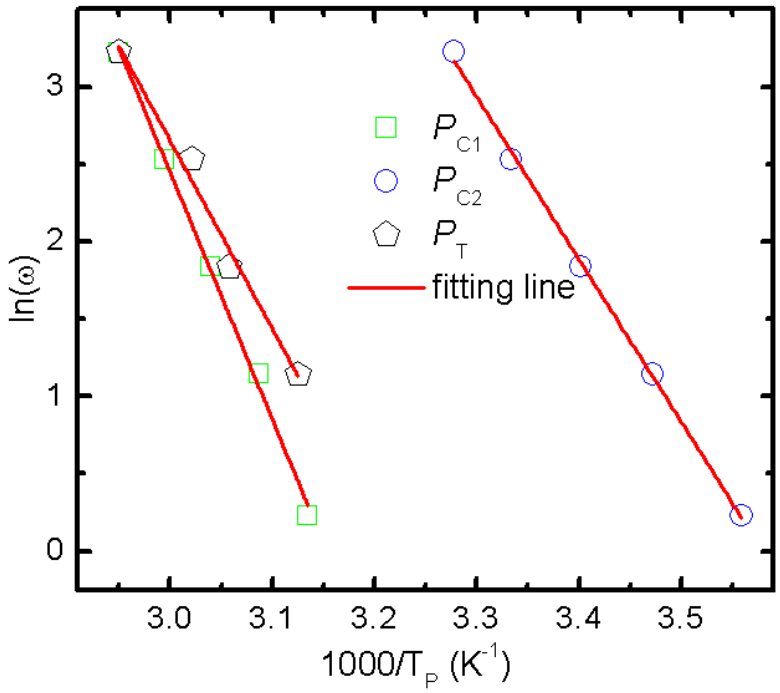

Physical Chemistry Chemical Physics Accepted Manuscript

Figure 10 by X. P. Wang, *et al*

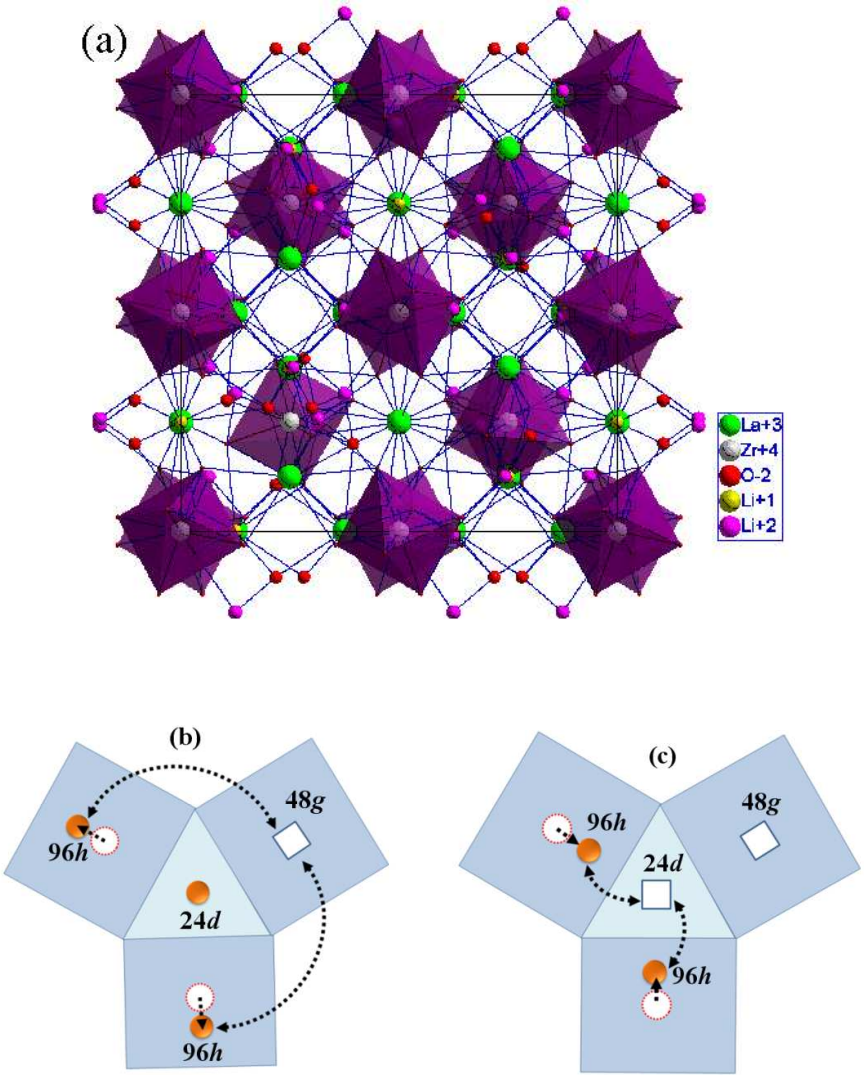

Physical Chemistry Chemical Physics Accepted Manuscript

Figure Captions

Figure 1: (a) The room temperature X-ray diffraction patterns for the tetragonal $Li_7La_3Zr_2O_{12}$ and the 10%Al-stablized cubic $Li_7La_3Zr_2O_{12}$, respectively; (b) The observed, calculated, Bragg positions and deference of the Rietveld refinement from the X-ray diffraction patterns of cubic $Li_7La_3Zr_2O_{12}$ using a space group *Ia-3d*. Insert in Fig.1(a): The enlarged local comparison between the cubic and tetragonal phase, and obvious tetragonal splitting is observed as evidenced by the diffraction (213) and (426) lines.

Figure 2: Impedance spectra of Al doped cubic $Li_7La_3Zr_2O_{12}$ at four different temperatures: (a) t=55 ^oC; (b) t=300 ^oC; (c) t=400 ^oC; (d) t=500 ^oC.

Figure 3: Temperature dependence of total ionic conductivity for the Al-stabilized and undoped tetragonal $Li_7La_3Zr_2O_{12}$ compounds and the activation energies of lithium ion migration are 0.36 eV for the Al containing compound.

Figure 4: Temperature dependence of the internal friction (Q^{-1}) and the relative modulus (M) for the Al stabilized $Li_7La_3Zr_2O_{12}$ sample measured at five different frequencies (0.2, 0.5, 1, 2 and 4 Hz) with a heating rate of 2 K/min.

Figure 5: Temperature dependence of the internal friction (Q^{-1}) of the Al stabilized $Li_7La_3Zr_2O_{12}$ sample under four different experimental strains, which demonstrates that the internal friction spectra are independent on strain magnitude.

Figure 6: The spectra of internal friction (Q^{-1}) and the relative modulus (M) of the tetragonal $Li_7La_3Zr_2O_{12}$ at four different frequencies (0.2, 0.5, 1, 2 and 4 Hz) with a heating rate of 2 K/min.

Figure 7: Comparison of internal friction spectra of the tetragonal and cubic $Li_7La_3Zr_2O_{12}$ at 1 Hz.

Figure 8: (a) Schematic of single Debye peak, which is obviously narrower than peak P_C; (b) Double peak fitting results of peak P_C based on the coupling model, the circles are experimental data points, the dot line is fitting background, the dash and dash-dot lines are the fitting P_{C1} and P_{C2} peaks, respectively.

Figure 9: The Arrhenius plots of the two relaxation sub-peaks (P_{C1} and P_{C2} peaks) in the cubic phase and P_T peak in the

Physical Chemistry Chemical Physics Accepted Manuscript

tetragonal phase, respectively.

Figure 10: (a) Crystal structure model for cubic $Li_7La_3Zr_2O_{12}$ projected on (001) direction (space group *I*a-3*d*). (b) Possible migration routes of lithium ions via 96*h*↔48*g*; (c) Possible migration routes of lithium ions via 24*d*↔96*h*. The yellow balls are occupied lithium ions, and the open circles and squares are proposed lithium vacancies.

Physical Chemistry Chemical Physics Accepted Manuscript